

ANALYSIS AND OPTIMIZATION OF *SPIRULINA PLATENSIS* MICROBIAL FUEL CELL

A Thesis

by

NICOLE ANN LONGTIN

Submitted to the Office of Graduate and Professional Studies of
Texas A&M University
in partial fulfillment of the requirements for the degree of
MASTER OF SCIENCE

Chair of Committee,	Sandun Fernando
Committee Members,	Carmen Gomes
	Kung-Hui Chu
Head of Department,	Stephen Searcy

August 2019

Major Subject: Biological and Agricultural Engineering

Copyright 2019 Nicole Longtin

ABSTRACT

In the search for renewable energy alternatives to traditional energy sources, microbial fuel cells are emerging as a potential solution. MFCs can produce electricity while simultaneously treating wastewater or powering a biosensor. The algae *Spirulina platensis* was used due to its high nutritional content and ease of cultivation. A unique configuration that allows utilizing O₂ generated via photosynthesis at the cathode (targeting fuel cell operation in an oxygen-limited environment) for an algae-based microbial fuel cell was designed, developed, and tested for 21 days. The results showed the highest performance on day seven during the exponential growth phase, with an open circuit voltage of 227.7 ± 0.08 mV. The highest power density was obtained when the fuel cells were connected in parallel, at 59.8 ± 7.96 mW/cm². Electrochemical Impedance studies helped to characterize the bonding events of the biofilm on the anode. It was determined that the equivalent circuitry of the fuel cell most closely resembled a Randles circuit. The biofilm growth on the anode increased the charge transfer resistance in the nine days measured. It was determined that for optimal output of the algal microbial fuel cell, fresh media should be added on the 14th day to keep *Spirulina platensis* in the exponential growth phase. If multiple fuel cells are run, they should be connected in series; however, the voltage from each needs to be equivalent to avoid any voltage reversal.

DEDICATION

To my Grandfather, Phillip Moore, for showing me the value of hard work and helping others.

You were, and continue to be, an inspiration to me in all that I do, always encouraging me to
strive for greatness.

To my parents, Doug and Helen Longtin, and my brother, Daniel Longtin, for the consistent and
unconditional love that you have shown me and for instilling in me the value of perseverance and
commitment.

To the rest of my family, for loving and supporting me, my success would not be possible without
it.

ACKNOWLEDGMENTS

First and above all else, I would like to thank God, without whom nothing would be possible.

Next I would like to thank my committee chair, Dr. Sandun Fernando, for all of his support, guidance, and encouragement throughout the course of this research. I would also like to thank the rest of my committee, Dr. Carmen Gomes and Dr. Kung-Hui Chu for their support and advice. Next, thanks goes to my lab group, specifically Varun Gejji, Aishwarya Mahadevan, and Nalin Samarasinghe for being so patient to answer all my questions and assist me unconditionally. Thanks to Daniela Oliveira for her guidance and assistance with my research.

Thanks also go to all of my friends for their love, encouragement and support. For inspiring me in my faith, celebrating me in all my achievements, and filling this journey with joy and laughter. Specifically I would like to thank all of the incredible women I have lived with during my time as a graduate student, Caroline Richard, Tevah Beller, Karina Morales, Jordan Warren, Amanda Kiecke, Alex Donaldson, Hope Valle, Morgan Bass, Samantha Duffey and Caitlin Wheat. Thank you to the women who have stood by me as my close friends, Lauren Ehle, Audrey Villarreal, Rebecca Quartemont, Megan Terry, Elissa Estep, Kaylin Perdomo, Annie DeFrees and Kelley Malone. Lastly, thank you to the families who have loved me like I was one of their own, the Flippens, Puceks, and Tuckers.

CONTRIBUTORS AND FUNDING SOURCES

Contributors

This work was supported by a thesis committee consisting of Professor Dr. Sandun Fernando of the Department of Biological and Agricultural Engineering and Professor(s) Dr. Carmen Gomes of the Department of Mechanical Engineering at Iowa State University and Dr. Kung-Hui Chu of the Department of Civil Engineering.

All other work conducted for the thesis was completed by the student independently.

Funding Sources

Graduate study was supported in part by Texas A&M Agrilife.

NOMENCLATURE

PEM	Proton Exchange Membrane
PEMFC	Proton Exchange Membrane Fuel Cell
EFC	Enzymatic Fuel Cell
DMFC	Direct Methanol Fuel Cell
MFC	Microbial Fuel Cell
PAFC	Phosphoric Acid Fuel Cell
AQDS	Anthraquinone-2,6-disulfonate
OCV	Open Circuit Voltage
COD	Chemical Oxygen Demand
SEM	Scanning Electron Microscopy
EIS	Electrochemical Impedance Spectroscopy
TGA	Thermogravimetric Analysis
CV	Cyclic Voltammetry

TABLE OF CONTENTS

	Page
ABSTRACT.....	ii
DEDICATION.....	iii
ACKNOWLEDGMENTS.....	iv
CONTRIBUTORS AND FUNDING SOURCES.....	v
NOMENCLATURE.....	vi
TABLE OF CONTENTS.....	vii
LIST OF FIGURES.....	ix
LIST OF TABLES.....	xi
1. INTRODUCTION AND LITERATURE REVIEW.....	1
1.1 Fuel Cell.....	1
1.1.1 Direct Methanol Fuel Cell.....	4
1.1.2 Acid Fuel Cell.....	5
1.1.3 Microbial Fuel Cell.....	6
1.1.3.1 Bacterial Microbial Fuel Cell.....	7
1.1.3.2 Fungal Fuel Cell.....	8
1.1.3.3 Algal Fuel Cell.....	8
1.1.4 Algal Fuel Cell.....	9
1.1.4.1 Types of Algae.....	9
1.1.4.2 Configurations.....	11
1.2 Overall Objective.....	12
2. ALGAL FUEL CELL.....	13
2.1 Introduction.....	13
2.2 Preliminary Work.....	13
2.3 Methods and Materials.....	14
2.3.1 Algae Growth.....	14
2.3.2 Growth Curve.....	14
2.3.3 Anode Surface Area.....	14
2.3.4 Algal Fuel Cell Potential Voltage.....	15
2.3.5 Algal Fuel Cell Standard.....	17

2.4	Results and Discussion.....	18
2.4.1	Algae Growth.....	18
2.4.1.1	Growth curve	18
2.4.2	Fuel Cell	20
2.4.2.1	Surface area analysis.....	20
2.4.2.2	Open circuit polarization curve and power curve (Characteristic curves)	21
2.4.2.3	Closed circuit polarization curve and power curve.....	24
3.	ELECTROCHEMICAL ANALYSIS OF ALGAL FUEL CELL	27
3.1	Introduction	27
3.2	Methods and Materials.....	30
3.2.1	Electrochemical Impedance Spectroscopy	30
3.2.2	SEM Images.....	30
3.3	Results and Discussion.....	30
3.3.1	Scanning Electron Microscopy images.....	33
4.	SUMMARY AND CONCLUSIONS.....	36
4.1	Future Work	37
	REFERENCES	38

LIST OF FIGURES

FIGURE	Page
1.1 Simple Direct methanol fuel cell fuel cell schematic.....	3
1.2 Acid Fuel Cell basic schematic.....	5
1.3 Microbial fuel cell basic schematic.....	6
2.1 Schematic of algae fuel cell used for all testing with <i>Spirulina platensis</i> in the anode compartment.....	16
2.2 Individual, series and parallel circuit configurations with ammeter and resistor	18
2.3 Growth curve of <i>Spirulina platensis</i> showing the absorbance and the concentration of algae with respect to days since inoculation in Zarrouk's media.....	19
2.4 Cyclic Voltammogram of the ferricyanide redox reaction at various scan rates to calculate surface area.....	20
2.5 Randles-Sevcik equation plot showing the current maximum versus the square root of scan rate.....	21
2.6 Polarization curve overlay showing days 2, 4, 7, 9, 14 and 21.....	22
2.7 Potential power curve overlay comparing output from different days, inset picture shows smaller range.....	23
2.8 Polarization curve comparing algal fuel cell in parallel, series, and individual configurations.....	24
2.9 Power curve comparing algal fuel cell in parallel, series, and individual configurations.....	25
3.1 Nyquist plot.....	29
3.2 Nyquist plots obtained on days 2, 4, 7 and 9 of algal fuel cell testing. Inset picture shows the semi-circle at high frequency range indicating charge transfer resistance. ...	31
3.3 Randles circuit showing solution resistance (R_s), charge transfer resistance (R_{CT}), double layer capacitance (C_{dl}) and Warburg impedance (Z_w).....	32

3.4 SEM image of the bare graphite felt electrode at 200μm and inset shows at 20μm 33

3.5 (a) SEM image of *Spirulina platensis* biofilm on the surface of a graphite felt electrode, coated with gold for imaging at 200μm and the inset at 100μm. 34

LIST OF TABLES

TABLE	Page
1.1 Comparison of DFMC, acid fuel cell and MFC.....	3
1.2 Comparison of various bacteria used in MFCs with their substrates, mediators and power output.....	7
1.3 Comparison of <i>Chlorella spp.</i> and <i>Spirulina spp.</i>	10
3.1 AC Impedance Parameters	30
3.2 Solution resistance and charge transfer resistance on days 2, 4, 7 and 9 of an algal-based microbial fuel cell.	32

1. INTRODUCTION AND LITERATURE REVIEW

With the world population steadily increasing, and the availability of affordable fuel sources diminishing, research into renewable fuel sources is vital. Currently, the most broadly used energy sources are derived from fossil fuels, even though these sources will be depleted within the next 50-100 years [1]. In addition to the concerns over the depletion of current energy sources, there is rising concern over the detrimental effects that fossil fuels have on the environment. The growing population, estimated by the United Nations to be at 9.8 billion by 2050, adds further pressure to the already dire need for additional and renewable energy sources [2]. The general scientific consensus is that no single energy source or solution is sufficient to meet the world's energy needs. A multifaceted approach is needed to alleviate this energy crisis [3].

There are many potential solutions to this energy crisis that needs to be further investigated. In 2015 the International Energy Agency reported that 10% of the world's total primary energy supply is from biofuels and waste, 2.4% is from water and 1.1% from other renewable sources like wind and sun [4]. This report shows that the emphasis that our world places on renewables in its current sustainable energy practices is not sufficient and that there is room for growth in the renewable sector.

1.1 Fuel Cell

Fuel cells have the potential to be a solution to this sustainable energy problem. Fuel cells are devices that convert the chemical energy stored in bonds into electrical energy through electrochemical reactions [5]. The fuel cell itself is not consumed as it produces electricity, but it continues producing electricity so long as it has a fuel source. Fuel cells work by harnessing electrons as they move from high-energy reactant bonds to low-energy product bonds. The electric current is created by separating the reactants so the electron transfer is done over an

extended length [6]. The basic configuration of a fuel cell consists of two electrodes, the anode and cathode, separated by a proton exchange membrane (PEM). The fuel source is in the anode compartment where the reaction occurs. The electrons are transferred across a load to the cathode and the protons travel through the PEM to the cathode compartment where they combine with oxygen to produce water. Fuel cells are being researched heavily due to their ability to produce clean, renewable electricity. They are being explored for use in many practical applications. Alkaline fuel cells were used in space missions because they could provide reliable electricity, were low weight, inexpensive, and produced potable water [7]. Proton exchange membrane fuel cells (PEMFCs) have been used in transportation systems due to their quick start up, sustained operation at high current density, and compactness [8]. Finally, enzymatic fuel cells (EFCs) could be used in portable medical devices or biosensors due to their potential power density, compactness, and the ability to be operated at room temperature [9]. There are many other types of fuel cells, utilizing different fuel sources and reactants. Some of the most common types to be discussed here are direct methanol fuel cells (DMFCs), acid fuel cells, and microbial fuel cells (MFC). A comparison of their advantages, disadvantages, and potential applications can be found in Table 1.1.

Table 1.1: Comparison of direct methanol fuel cell, acid fuel cell and microbial fuel cell.

Type	Microorganism	Advantages	Disadvantages	Applications	Reference
Direct Methanol Fuel cell	N/A	-High energy density -Quick refueling	-Technical barriers to improvement: methanol crossover, water management, and oxygen transport etc. -Produces minor amounts of CO ₂	-Portable power for consumer electronics -Transportation	[10] [11]
Acid Fuel Cell	N/A	-CO ₂ rejecting -High theoretical cell potential -Large scale up with reliability	-Best operation is above room temperature (150-250°C) -High cost for large scale facilities	-Portable power for consumer electronics -Power plants	[12] [13] [14]
Microbial Fuel Cell	-Bacterial	-Reducing BOD/COD	-Low power production	-Biosensors -Wastewater treatment	[15]
	-Fungal	-Easy cultivation	-Low power production -High cost at large scale -Most require electron mediator	-Wastewater treatment	[16]
	-Algal	-CO ₂ sequestering -Breaks down organic material	-Low power production	-Wastewater treatment -Space travel	[17]

1.1.1 Direct Methanol Fuel Cell

The DMFC schematic can be seen in Figure 1.1. It consists of an anode compartment where methanol is oxidized to CO₂ and a cathode compartment where oxygen is reduced to water [18].

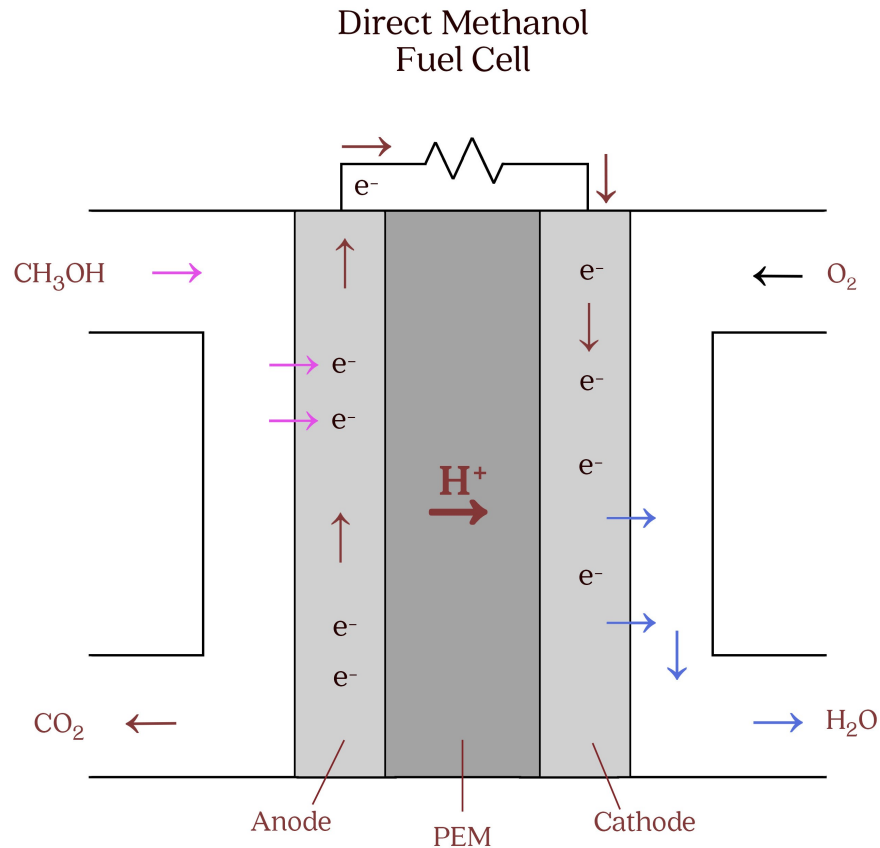
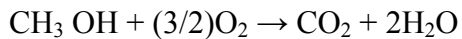


Figure 1.1: Simple Direct methanol fuel cell schematic.

The overall reaction being:



The DMFC is being explored primarily for use as portable power in consumer electronics [11]. If most of the technical barriers can be overcome, then the DMFC could eventually replace traditional rechargeable lithium batteries. The biggest changes that need to be made are in the

miniaturization of the fuel cell to fit in electronics, and increasing energy density without higher losses due to methanol crossover [10].

1.1.2 Acid Fuel Cell

Acid fuel cells follow the same major principle of DMFCs where a fuel source is added to the system, oxidized at the anode and reduced at the cathode to produce electricity and water [19]. The difference is that the membrane separating the anode and cathode compartments is an electrolyte, and the fuel source is hydrogen gas. The electrolyte acts as a proton conductor and transports the protons from the anode to the cathode [14]. Thus the overall reaction for this system is



The basic configuration of an acid fuel cell is in Figure 1.2. One of the most commonly used electrolytes for acid fuel cells is phosphoric acid (PAFC). The PAFC has been used in industrial and commercial settings for decades with high reliability, efficiency, and flexibility. The biggest barrier to overcome with PAFC is the high costs associated with scale up [14].

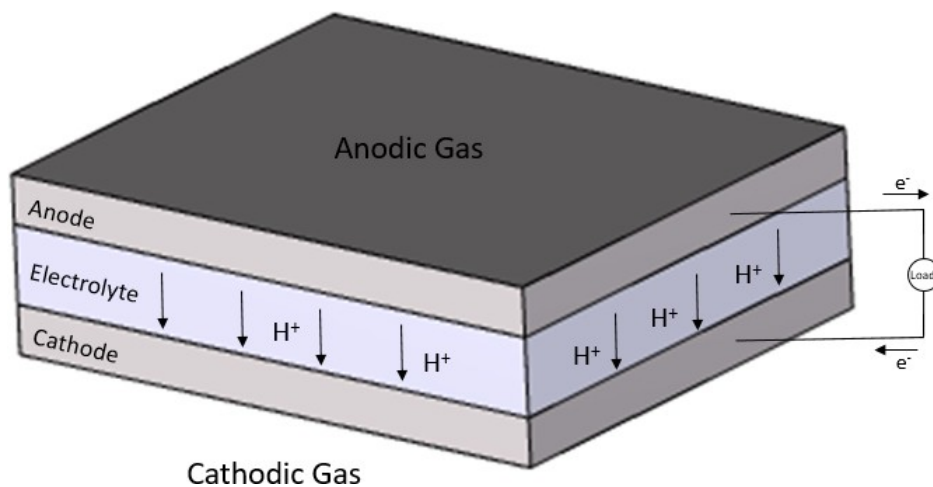


Figure 1.2: Acid Fuel Cell basic schematic.

1.1.3 Microbial Fuel Cell

Microbial fuel cells (MFCs) are one of the emerging fuel cell technologies being investigated. MFCs are being researched extensively due to their ability to produce clean, renewable electricity at room temperature while also having the potential for wastewater remediation. MFCs work similarly to the previous fuel cells, but they convert the chemical energy stored in the bonds of organic material into electrical energy through reactions of microorganisms [20]. Figure 1.3 shows the basic configuration of a microbial fuel cell.

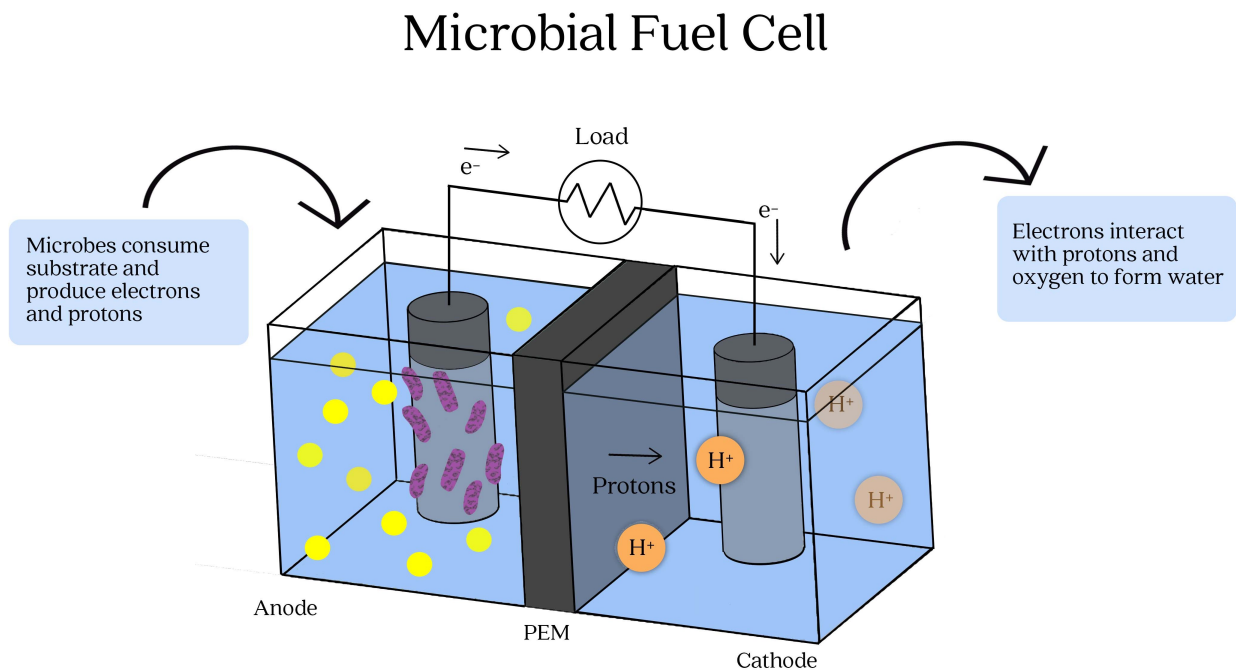


Figure 1.3: Microbial fuel cell basic schematic.

There are many possible applications of MFCs currently being explored. The most prominent applications are wastewater remediation, heavy metal removal, biosensors, and hydrogen production [17]. These applications are being investigated extensively due to their ability to provide bioelectricity from the output of the fuel cell while simultaneously meeting another need.

Since MFCs still have some challenges to overcome to increase output power, secondary uses for MFCs are beneficial in improving the practicality and efficiency of the MFC [21]. The microorganisms utilized in these fuel cells can be broken into three categories, bacterial, fungal and algal.

1.1.3.1 Bacterial Microbial Fuel Cell

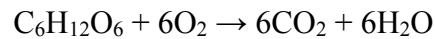
There are many strains of bacteria that have been used as the microbe in MFCs, as well as some MFCs with mixed cultures of bacteria. Some of the most common bacteria used are *Escherichia coli*, *Geobacter sp.*, *Schwanella sp.*, and *Clostridium sp.* [22]. With some species of bacteria, an electron mediator is required to transport the electrons to the anode [20]. The need for an electron mediator is one of the challenges to overcome with practical and cost-effective use of bacteria in MFCs. Table 1 shows some of the most common bacteria used in MFCs, along with their substrates and mediators.

Table 1.2: Comparison of various bacteria used in MFCs with their substrates, mediators and power output.

Type	Substrate	Mediator	Reference
<i>Escherichia coli</i>	-Glucose	-Methylene blue	[23]
<i>Geobacter ssp.</i>	-Acetate	-Carboxyl group modification	[24]
		-Mediator-less	[25]
<i>Schwanella ssp.</i>	-Lactate	-Mediator-less	[26]
		- Anthraquinone-2,6-disulfonate (AQDS)	[27]
<i>Clostridium ssp.</i>	-Starch	-Polytetrafluoroaniline	[28]
	-Glucose		
	-Lactose		

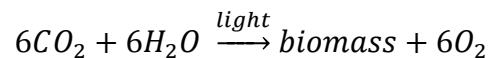
1.1.3.2 Fungal Fuel Cell

Fungi-based microbial fuel cells have been researched less than traditional bacterial MFCs due to lack of proven fungal electrogens. The most intensively investigated system for fungal MFCs is yeast-based. The yeast-based fuel cell has the advantage of being easy to grow, non pathogenic, and can metabolize a variety of substrates [16] [29] [30]. The overall reaction equation for the yeast based fuel cell is:



1.1.3.3 Algal Fuel Cell

One of the relatively newer microbes being extensively researched with regard to MFCs is algae. Algae are photosynthetic organisms that live in fresh or saltwater environments. Compared to other plants, they are better able to adapt their biochemical metabolic pathways in response to external conditions, making them a good fit for MFCs [31]. Their growth is influenced by a number of factors, nutrient quality and quantity, pH, temperature, light supply, dissolved oxygen and CO₂, and the presence of toxic elements in the medium [32]. Algae is a good alternative for bacteria and fungi in MFCs because they are generally photosynthetic and autotrophic, grow well in natural environments and produce large amounts of biomass that can be harvested for its nutritional content or other kinds of fuel [33]. Algae is also beneficial because it sequesters CO₂ as it undergoes photosynthesis and creating more biomass. The overall reaction taking place is:



This reaction can be broken up into 4 phases, light adsorption, electron transport, generation of ATP and carbon fixation. In the first phase, which is in the presence of light, the algae splits water into oxygen, protons and electrons. In the final phase the ATP⁺ and the NADPH provide the energy and electrons to drive the reaction ahead creating biomass and oxygen [34]. It is in the first phase of photosynthesis that the anode collects a portion of the electrons generated. Since the algae usually forms a biofilm on the anode, and most algae are naturally exoelectrogenic, they do not require an electron mediator to shuttle the electrons to the anode [35].

1.1.4 Algal Fuel Cell

1.1.4.1 Types of Algae

Several algal strains have been tested in microbial fuel cells with varying results. A table displaying the most commonly used strains and their performance in wastewater based microbial fuel cells was referenced [4]. The highest power densities came from *Chlorella vulgaris* (980mW/m²), *Scenedemus obiquus* (102mW/m²) and *Chlamydomonas reinhardtii* (78mW/m²). The highest open circuit voltage (OCV) came from *Chlorella vulgaris* (0.8V), *Spirulina platensis* (0.49V) and *Dunaliella tertiolecta* (0.49V). However, more factors than just power output should be considered in selecting the algae strain to be used in various applications. Depending on the goals of the project, factors like cost, growth rate, chemical oxygen demand (COD) removal efficiency, power output, and growth conditions should be considered [36]. The two strains to be compared here are *Chlorella* and *Spirulina*. Table 1.3 shows the differences of *Chlorella sp.* and *Spirulina sp.* in nutrient content, performance, and cultivation.

Table 1.3: Comparison of *Chlorella spp.* and *Spirulina spp.*

Species	Nutrient Content			Performance		Cultivation	Reference
	Lipid%	Carbohydrate%	Protein%	% COD Removal	Power Density (mW/m ²)		
<i>Chlorella spp.</i>	2-46	12-28	11-58	73	30.15	Jaworski's Medium	[33] [37]
<i>Spirulina spp.</i>	4-9	8-16	46-63	67	20.5	Zarrouk's medium	[33] [4]

There are many factors to consider when choosing between different algae, depending on the intended application. The performance is usually slightly higher in fuel cells with *Chlorella* in both % COD removal and power density. However, *Spirulina* has a higher nutrient content, specifically % protein, and depending on the goal of the fuel cell, the difference in performance can be considered acceptable [33].

1.1.4.2 Configurations

The configuration of the microbial fuel cell plays an important role on fuel cell performance. Different configurations are typically used depending on the microbes and application of the fuel cell. There are two main configurations, single chamber and double chamber [20], [38].

The double chamber configuration is depicted in Figures 1.1, 1.2 and 1.3. It consists of two chambers separated by a membrane, which only allows for the transfer of protons. In a single chamber fuel cell, the anode and cathode are in the same solution with half of the cathode in solution and the other half exposed to air. There are advantages and disadvantages to both systems that must be considered in determining which configuration is best for the specific system. Typically for an algal fuel cell, the double chamber configuration is used [39]. However, research is being done examining the use of algae in both the anode and cathode compartments for different purposes. Algae have been used in the anode as a substrate for other exoelectrogenic bacteria and as the primary electron donor in what is also called a photosynthetic microbial fuel cell [40], [41], [42]. In the cathode, algae are used to produce oxygen as an electron acceptor and to capture the CO₂ produced. Lastly, algae have been used simultaneously in both the anode and cathode compartments to achieve multiple experimental and application goals such as increased performance and wastewater treatment [4].

1.2 Overall Objective

For the purpose of this study, a fuel cell that is easily fabricated, has moderate power output, can serve as a nutrient source, and can be operated in a wastewater treatment system is desired. Thus, an algae-based microbial fuel cell with *Spirulina platensis* was selected.

Specific Objective 1: To design, develop and test an algal fuel cell with microalgae in the anode compartment.

The key tasks associated with this Specific Objective are:

- Surface characterization of the anode by making a growth curve and getting SEM imagery of the bare anode and anode with biofilm growth. Calculating the surface area of the anode using cyclic voltammetry and the Randles-Sevcik equation.
- Evaluate fuel cell performance through the execution of a resistor sweep and creating polarization and power curves.

Specific Objective 2: To perform electrochemical impedance analysis of fuel cell to evaluate binding events on the anode.

The key tasks associated with this Specific Objective are:

- To perform electrochemical impedance spectroscopy analysis in order to obtain Nyquist plots.
- To characterize fuel cell anode by identifying an equivalent circuit model that best fits the EIS data.

2. ALGAL FUEL CELL

2.1 Introduction

As previously described, there is a great need for advancement in renewable technologies. Algae-based MFCs could be a great alternative to traditional fuel sources. An algal fuel cell could be used for wastewater treatment and energy generation. The optimization of an algae-based fuel cell is needed before it can be utilized on a commercial scale. This chapter discusses the methods and materials used to develop and test the algae-based microbial fuel cell. It also includes the results of the tests and analysis.

2.2 Preliminary Work

The MudWatt fuel cell was adapted for use in this experiment. The mud in MudWatt fuel cells is used as the proton exchange membrane. However, to use this as an algal fuel cell, a substitution was needed to separate the anode and cathode compartments. With the goal of the final algae fuel cell being inexpensive to construct, a cost-effective PEM was desired. For the PEM to be successful, it must be able to separate the anode and cathode compartments but still allow the travel of protons. One design consideration was to use oxygen generated in the fuel cell anode on its own cathode. And, the MudWatt fuel cell's unique design of the anode sitting below the PEM and cathode allowed this requirement by permitting the oxygen in the anode compartment to diffuse to the top and become an end terminal electron acceptor. A basic household sponge, non-antimicrobial, was tested at varying thicknesses for optimization. The fuel cells were set up with yeast as the microorganism and glucose as the substrate. The thicknesses tested were 0.35in, 0.70in, and 1in. The fuel cell was run for 8 hours. The results showed that the thinnest sponge did not adequately separate the compartments and the OCV was too low to measure. The thickest sponge adequately separated the compartments but did not allow for easy proton transport and

thus the OCV was decreased. This preliminary study showed that the optimal thickness for the sponge membrane is 0.70-0.75in.

2.3 Methods and Materials

2.3.1 Algae Growth

The algae used, *Spirulina platensis*, was purchased from the UTEX algae bank. Zarrouk's media [43] was used to grow the algae, and fresh media was added (10%w/v) every 14 days to maximize growth. White light was provided for 12 hours daily with a timer, and the algae was kept at room temperature. Lastly, the beakers were stirred once daily to ensure adequate light adsorption.

2.3.2 Growth Curve

The growth curve compares the concentration of algae to the days since inoculation. By plotting the growth curve, the four phases of growth: log, exponential, stationary and death phases can be identified for this species and in these conditions. It is expected that the exponential growth phase will produce the highest output voltage, so this phase needs to be identified. Two replicates of 200mL of media was inoculated with 10mL of algae. The algae was stirred with a stir bar continuously and the rest of the conditions were identical to normal growth conditions. The concentration of algae was calculated on days 0, 2, 4, 7, 9, 14 and 21 using Thermogravimetric Analysis (TGA). This process uses temperature to measure the changes in physical and chemical properties of the sample. The concentration was calculated by first dividing the water weight by the density of water, to obtain volume. Then, the concentration was calculated by dividing the biomass weight by the volume of water.

2.3.3 Anode Surface Area

The effective cross-sectional surface area of the anode was calculated using cyclic voltammetry

(CV) and the Randles-Sevcik equation (Equation 1) [44] [45]. By holding all values constant except the scanning rate, v , the surface area, A can be calculated.

$$i_p = 0.4463nFAC \left(\frac{nFvD}{RT} \right)^{\frac{1}{2}} \quad \text{Equation 1}$$

If the solution is at 25°C:

$$i_p = 268,600n^{\frac{3}{2}}AD^{\frac{1}{2}}Cv^{\frac{1}{2}} \quad \text{Equation 2}$$

where i_p is current maximum in amps,

n is the number of electrons transferred in the redox event (assumed to be 1),

A is the electrode area in cm^2 ,

F is Faraday Constant in C mol^{-1} ,

D is diffusion coefficient in cm^2/s ,

C is concentration in mol/cm^3 ,

v is scan rate in V/s ,

R is gas constant in $\text{J K}^{-1} \text{mol}^{-1}$ and T is temperature in K .

The redox reaction for the CV was in 0.1M KCl mixed with 5mM ferricyanide. Two hundred milliliters of solution was made and the anode was placed in the solution along with a counter electrode and a reference electrode [46]. The CV was run at scan rates of 5, 10, 20, 35, 50, 100, 150, 200 and 300mV/s. The current maximum, or the peaks in the CV, that correspond to the oxidation of ferricyanide, were plotted against the square root of the scan rate in V/s. The slope of the trendline created was plugged into the equation, and the effective surface area of the electrode was calculated.

2.3.4 Algal Fuel Cell Potential Voltage

The modified MudWatt fuel cell system was used for all experiments. Fifty milliliters of 2.7% w/v algae suspension was added to the fuel cell chamber. The graphite anode was placed atop the

suspension and allowed to saturate fully. A sponge of average 18.2mm thickness was placed on top of the anode and 80mL of Zarrouk's media was poured on top of the sponge, ensuring that the sponge is completely saturated and the liquid line is visible at the surface of the sponge. The graphite felt cathode was placed on the sponge allowing good contact of the bottom of the cathode to the saturated sponge. Figure 2.1 shows the setup of the algae fuel cell.

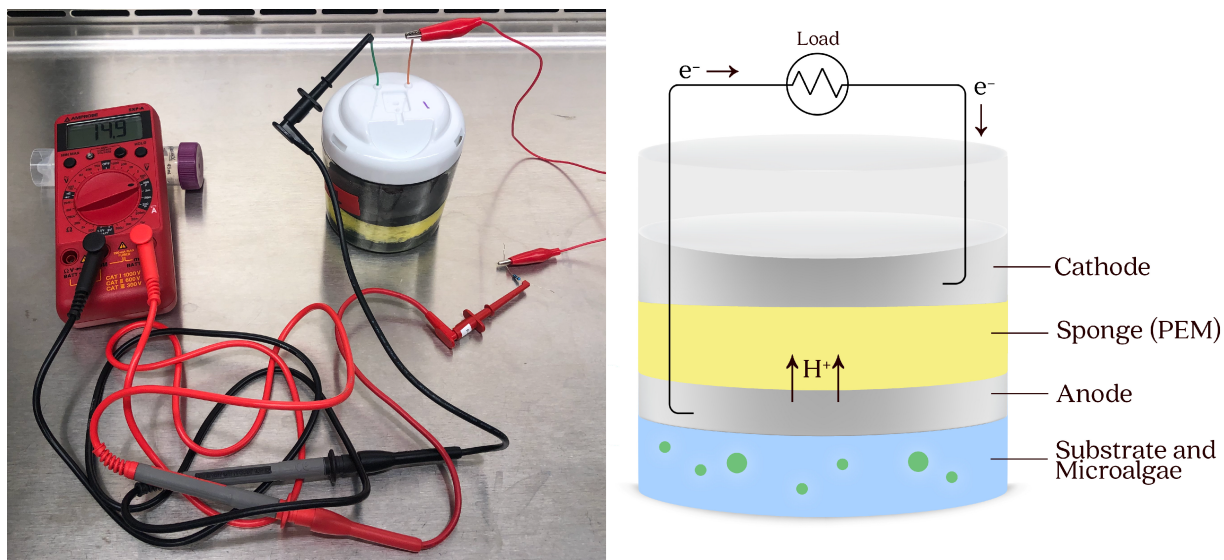


Figure 2.1: Schematic of algae fuel cell used for all testing with *Spirulina platensis* in the anode compartment.

The voltage measurements were taken with a multimeter. The open circuit voltage (OCV) was measured on days 0, 2, 4, 7, 9, 14 and 21 by connecting the multimeter directly to the anode and cathode wires. Starting on day 2, and continuing the rest of the days, the OCV along with resistor sweeps were measured. The resistors added were 1, 4.7, 10, 22, 47, 100, 220, 510, 1k, 10k, 33k, 75k, 1M, 1.5M, 5.6M, 10M ohms. The system was given 10 minutes to stabilize after each resistor was added before the voltage measurement was taken across the resistor.

Initially for collecting electrochemical data, the typical fuel cell circuit that consists of a

voltmeter fixed across the resistor was attempted. However, due to the low voltage and current in the system, likely due to the low cell densities during lag phase, no measurement could be taken. Therefore, the resistors were connected to the anode and the multimeter in series, which was attached to the other end of the resistor and the cathode. Measuring the voltage of the system along with resistance allowed measurement of OCV and potential power the fuel cell could generate (since no current is passing through the open circuit) for a given load. This setup allowed identification of the best conditions the fuel cell would operate under to develop proper characteristic curves. A polarization curve, which compares the voltage to the current density, was created next. Here it should be noted that the resistance used to calculate potential power did not include the internal resistance of the fuel cell. This procedure was considered adequate for performance comparison purposes. The current density was calculated using Ohm's law, $V=IR$. Thus, the theoretical current was calculated by dividing the voltage by the resistance added ($I=V/R$). Then the current density was found by dividing the current calculated by the effective cross-sectional surface area of the anode. The polarization curve is used to examine the ohmic losses in the system. The power and power density were calculated using Ohm's law, ($P=I^2R$) and dividing the calculated theoretical power by the effective cross-sectional surface area, respectively. This data was used to create a power curve, which compares the current density with the power density. The power curve was used to identify the potential maximum power output by the fuel cell with respect to current density.

2.3.5 Algae Fuel Cell Standard

In order to collect data in the standard way for fuel cells, the current was measured on the day with the highest output and the voltage was calculated using Ohm's law. The ammeter was connected in series with the fuel cell and the resistor. The same resistors were used to measure the change in current with increased resistance.

After each replicate was measured the three fuel cells were connected in parallel and in series

and the same resistor sweep was performed. Figure 2.2 shows the circuit of the fuel cell individually, in parallel and in series for current measurements with resistance.

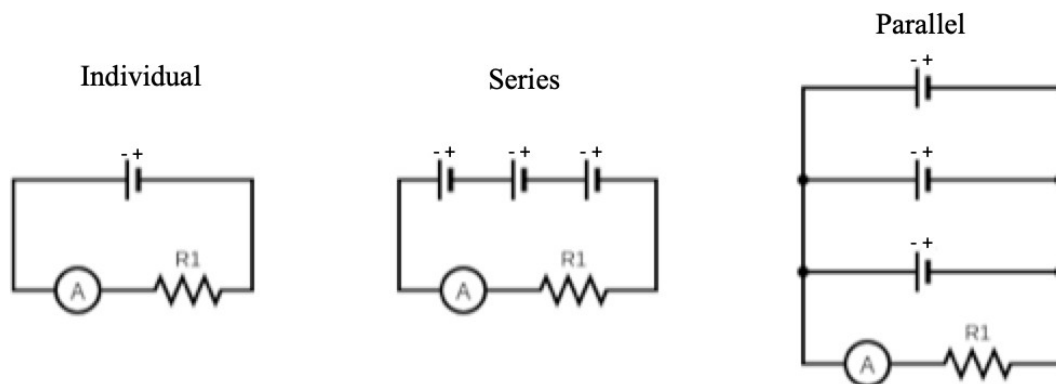


Figure 2.2: Individual, series and parallel circuit configurations with ammeter and resistor.

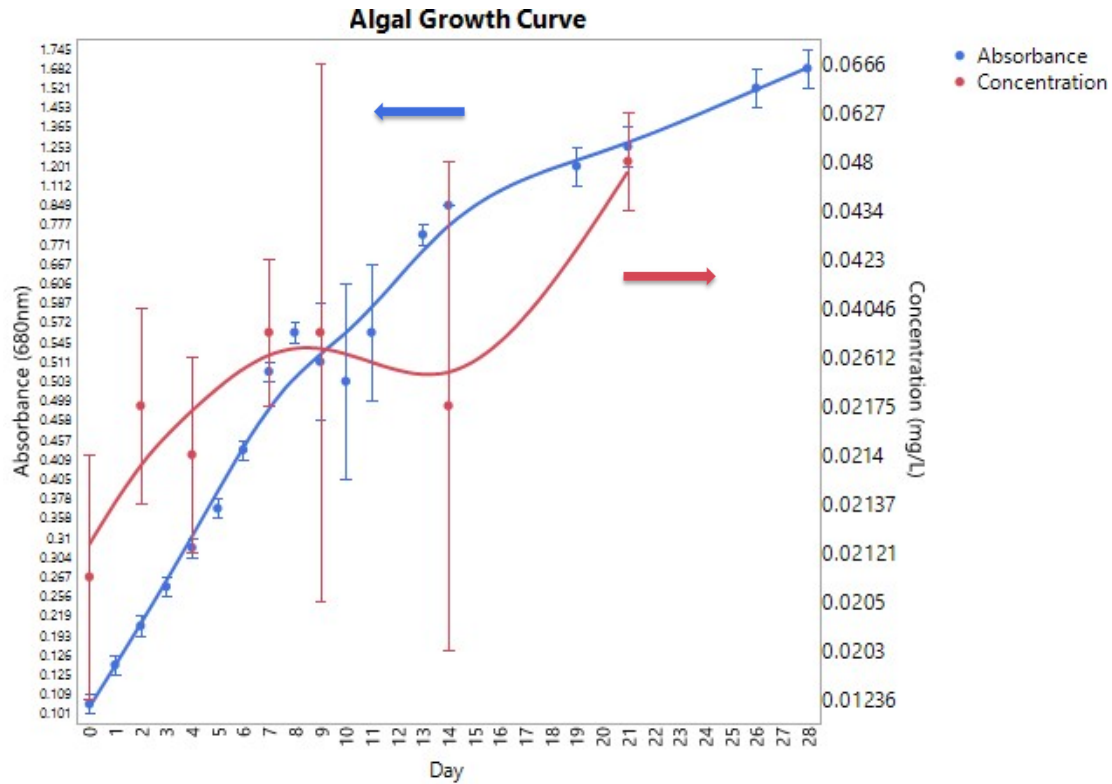
All experiments were analyzed as a completely randomized design with three replicates unless mentioned otherwise. The level of significance (α) was set at 0.05 for ANOVA testing.

2.4 Results and Discussion

2.4.1 Algae Growth

2.4.1.1 Growth curve

Figure 2.3 depicts the growth of *Spirulina platensis* daily through the absorbance and concentration measurements. There is a high error in the concentration measurements likely due to the sensitivity of the measurement type. The microalgae were forming clusters in the growth chamber even with constant stirring, thus there is a high chance of irregularity in such precise measurements.



Each error bar is constructed using 1 standard error from the mean.

Figure 2.3: Growth curve of *Spirulina platensis* showing the absorbance and the concentration of algae with respect to days since inoculation in Zarrouk's media.

The growth curve shows no noticeable lag phase, likely due to the fact that the algae was already in the same media that was used for inoculation. The adjustment period, or lag phase, would not be seen on the scale of days in this case. The exponential growth phase starts to decline around day 9. This is reflected in the results of the fuel cell characteristic curves. The life span of the algae was longer than expected, so absorbance measurements were taken to 28 days to fully capture the growth behavior. Another factor to consider in the growth curve is that with continual stirring the dead algae does not separate and there will be no decline in the graph because the total biomass in the media is still increasing.

2.4.2 Fuel Cell

2.4.2.1 Surface area analysis

In order to develop fuel cell characteristic curves the surface area of the electrode is necessary. Although the nominal surface area could be used for this, a more accurate measure is the active surface area. To calculate active surface area CV scan rates were generated at a constant concentration of potassium ferricyanide (Figure 2.4).

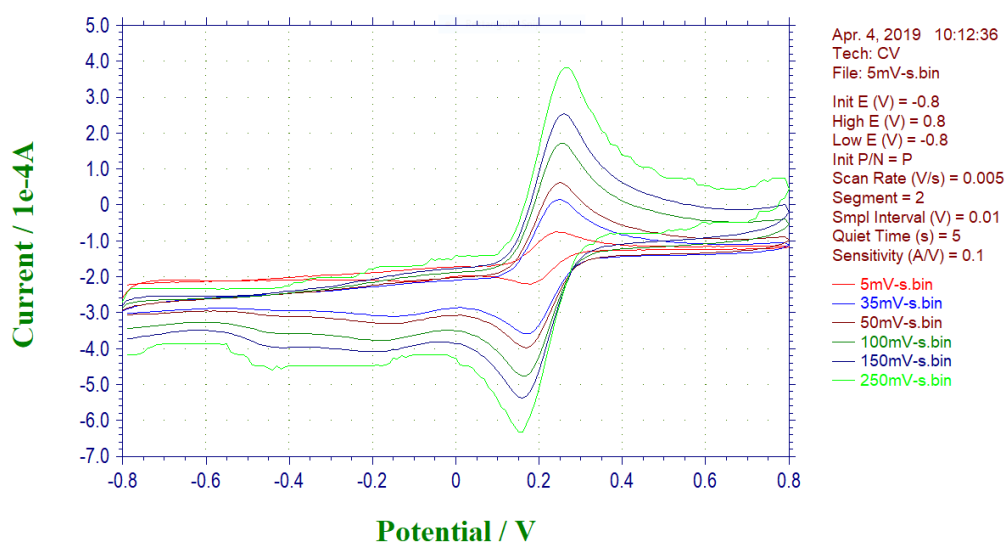


Figure 2.4: Cyclic Voltammogram of the ferricyanide redox reaction at various scan rates to calculate surface area.

The positive current peaks represent ferricyanide oxidation whereas negative currents depict reduction. The Cottrell plot of the current maximum and the square root of the scan rate that is needed for surface area calculation can be seen in Figure 2.5 along with the trendline.

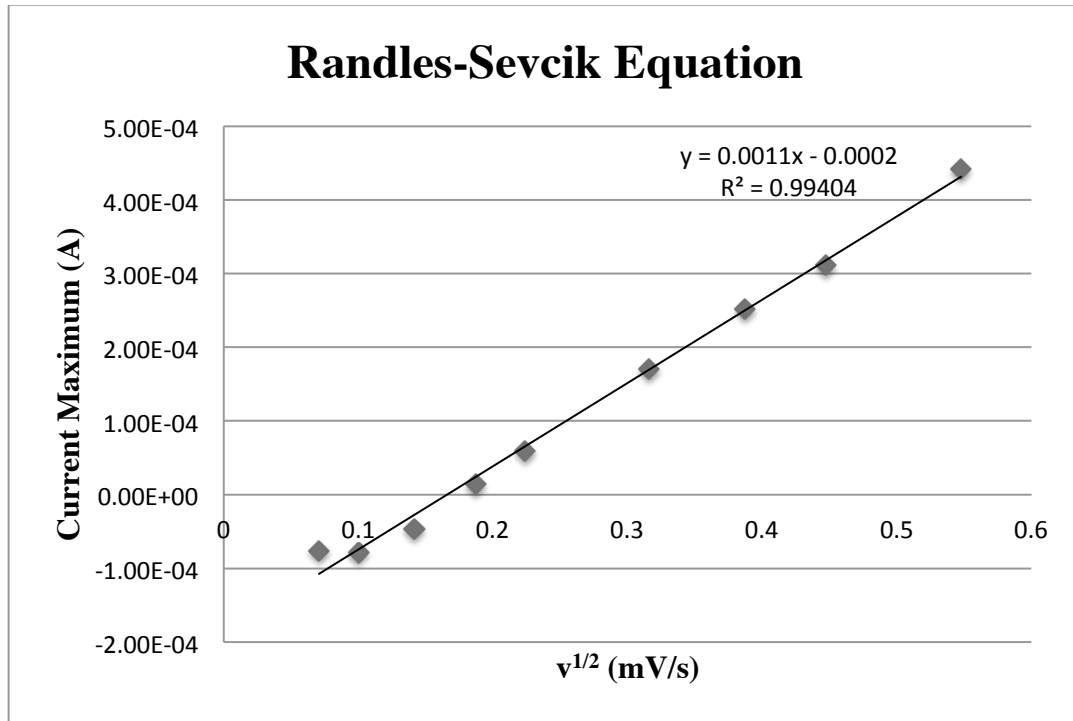


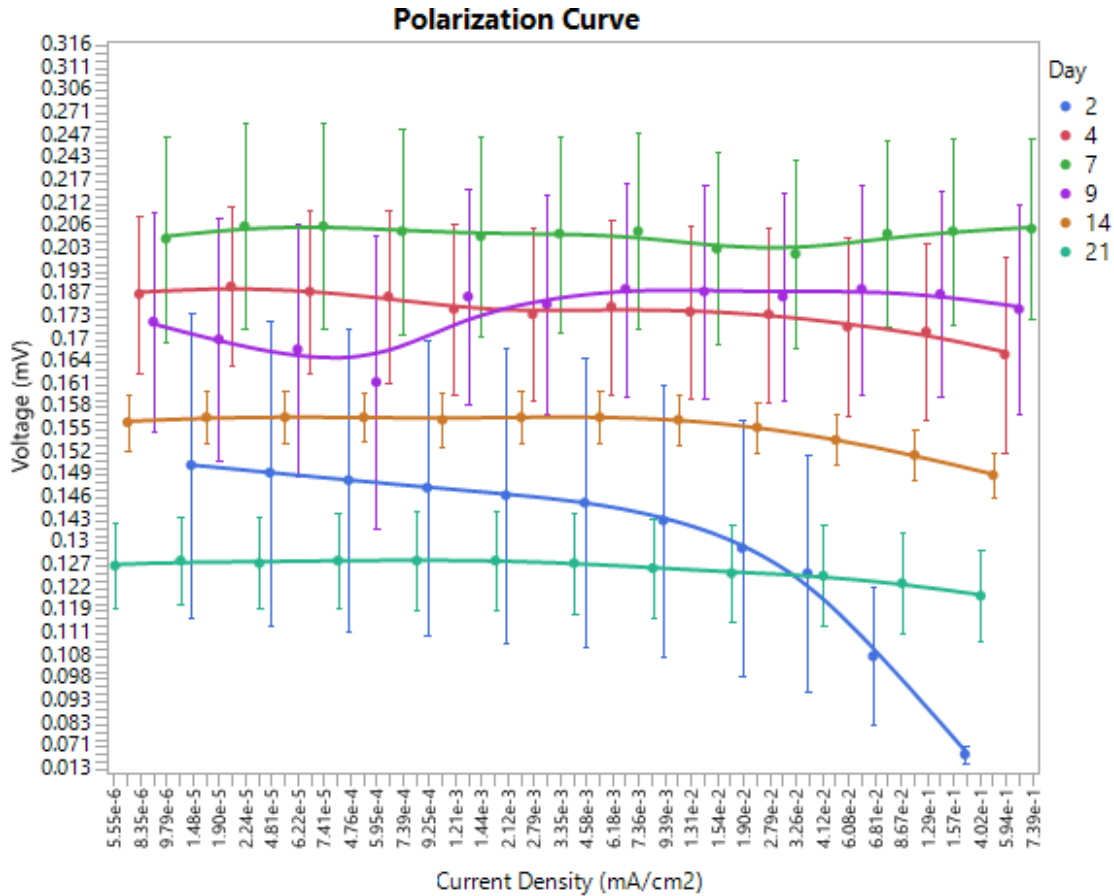
Figure 2.5: Randles-Sevcik equation plot showing the current maximum versus the square root of scan rate.

The effective surface area was calculated by setting the slope of the trendline (0.0011) equal to the slope of the Randles-Sevcik equation. The diffusion coefficient, $7.17\text{E-}6 \text{ cm}^2/\text{s}$ at the concentration 5mM as reported by Konopka and McDuffie [46] was used for the surface area calculation. The surface area was found to be 0.3061cm^2 . This number is lower than expected since the diameter of the anode is 8cm and the electrode is macro-porous. However, this method measures the effective surface area, meaning the area that is available for electrical interactions, and this value can be expected to be lower. The real surface area calculated, i.e., 0.3061cm^2 , was used for the current density and the power density calculations.

2.4.2.2 Open circuit polarization curve and power curve (Characteristic curves)

Since the voltage was too small to read using the standard method, the resistance was added between the anode and the multimeter. This measures the potential voltage while removing any ohmic losses. The resulting power curves could be used for comparing OCVs and potential power

generation by the fuel cell under different conditions. The polarization curve in Figure 2.6 compares cell performance on each of the days the resistor sweep was performed.

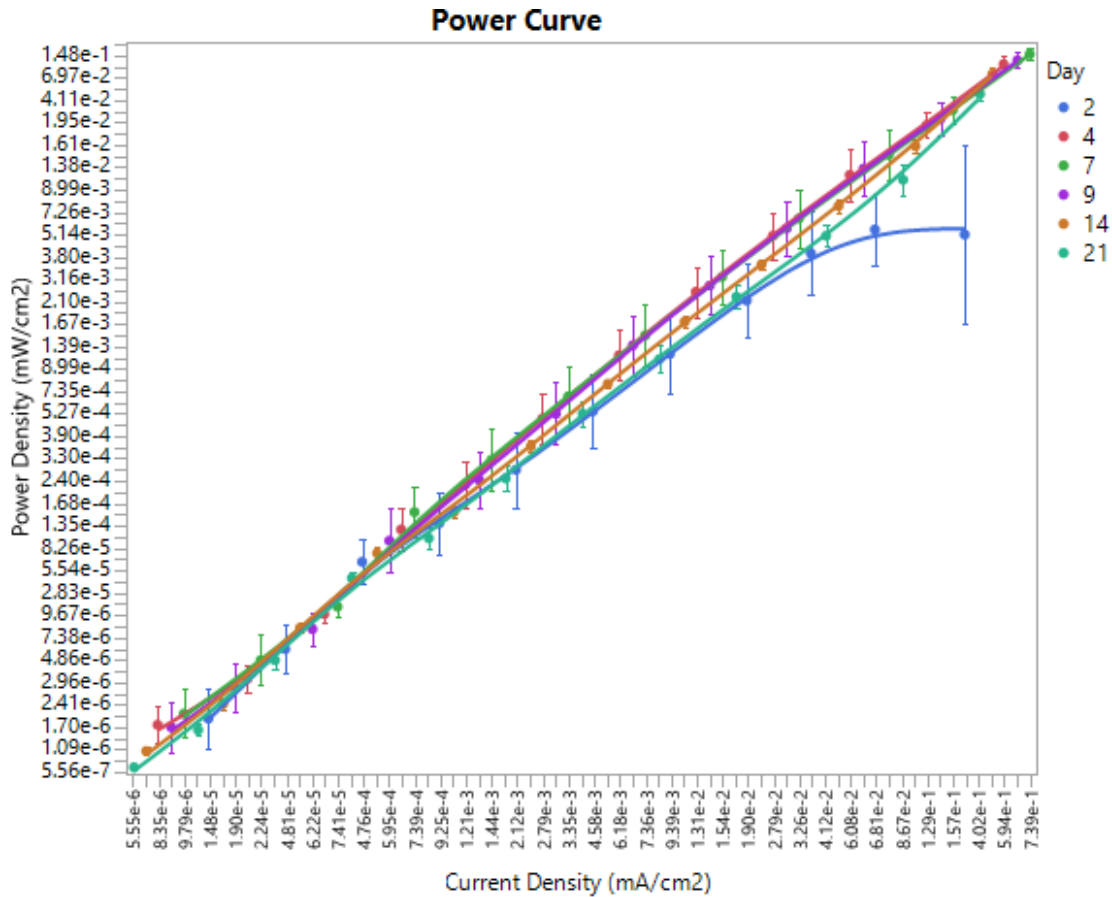


Each error bar is constructed using 1 standard error from the mean.

Figure 2.6: Polarization curve overlay showing days 2, 4, 7, 9, 14 and 21 for a resistor sweep with values ranging from 1Ω to 10MΩ.

This figure shows that the highest theoretical OCV output resulted on day 7 followed by days 4 and 9. This response is to be expected, as the algae should be in its exponential growth phase at this stage after inoculation. The graphs also do not show the typical drop in voltage with increasing current density as a result of the lack of typical ohmic losses. In retrospect, a closed circuit system where current flows would show losses due to the reaction rate, resistance, and gas transport. The potential power that could be generated from the cell under different conditions/days is given in

Figure 2.7. The p-value was under 0.0001 showing a significant trend between the OCV and days tested.



Each error bar is constructed using 1 standard error from the mean.

Figure 2.7: Potential power curve overlay comparing output from different days.

It can be noticed that the overlay does not show the typical expected parabolic power curve [4]. This is likely due to the circuitry that was used to circumvent current measurement. It is possible that the highest resistance used was not high enough to capture the full power curve of the system. Another possibility is that the normal parabolic trend is not possible when the voltage is measured in series rather than across the resistor.

These results show the potential performance of the fuel cell with minimal system losses; additionally, this method was effective in identifying the best performing days/conditions in order

to develop standard characterization curves. Based on the analysis, the cell performed best on or around day seven.

2.4.2.3 Closed circuit polarization curve and power curve

Figure 2.8 and 2.9 show the polarization and power curves for the algal fuel cell system when attached to the load measurement circuitry individually, three cells in series, and three cells in parallel.

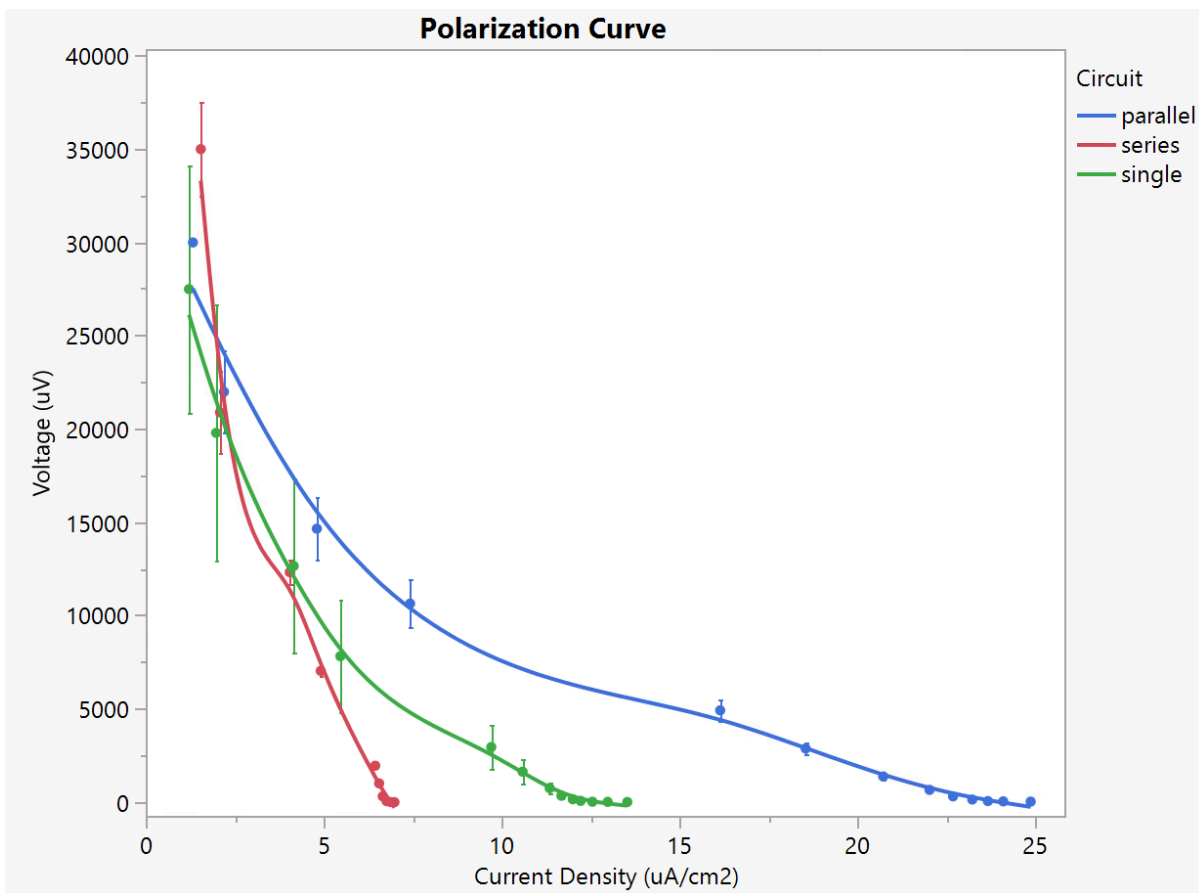


Figure 2.8: Polarization curve comparing algal fuel cell in parallel, series, and individual configurations.

The polarization curves depict that the voltages begin at $\sim 30\text{mV}$. As the current draw increased the voltage dropped as expected in a typical polarization curve. However, the polarization curve does not show the expected results for the three configurations. When the three fuel cells are put in series, it is expected for the voltages to add up and be higher across the resistor. However, the series curve showed the lowest output compared to the individual fuel cell and the ones connected in parallel. This is likely due to the voltage reversal phenomenon, where the overall voltage is reduced in series stacked MFCs. Voltage reversal happens when one of the cells in series has a lower output than the rest, and this has an adverse impact on the rest of the biofilms [47].

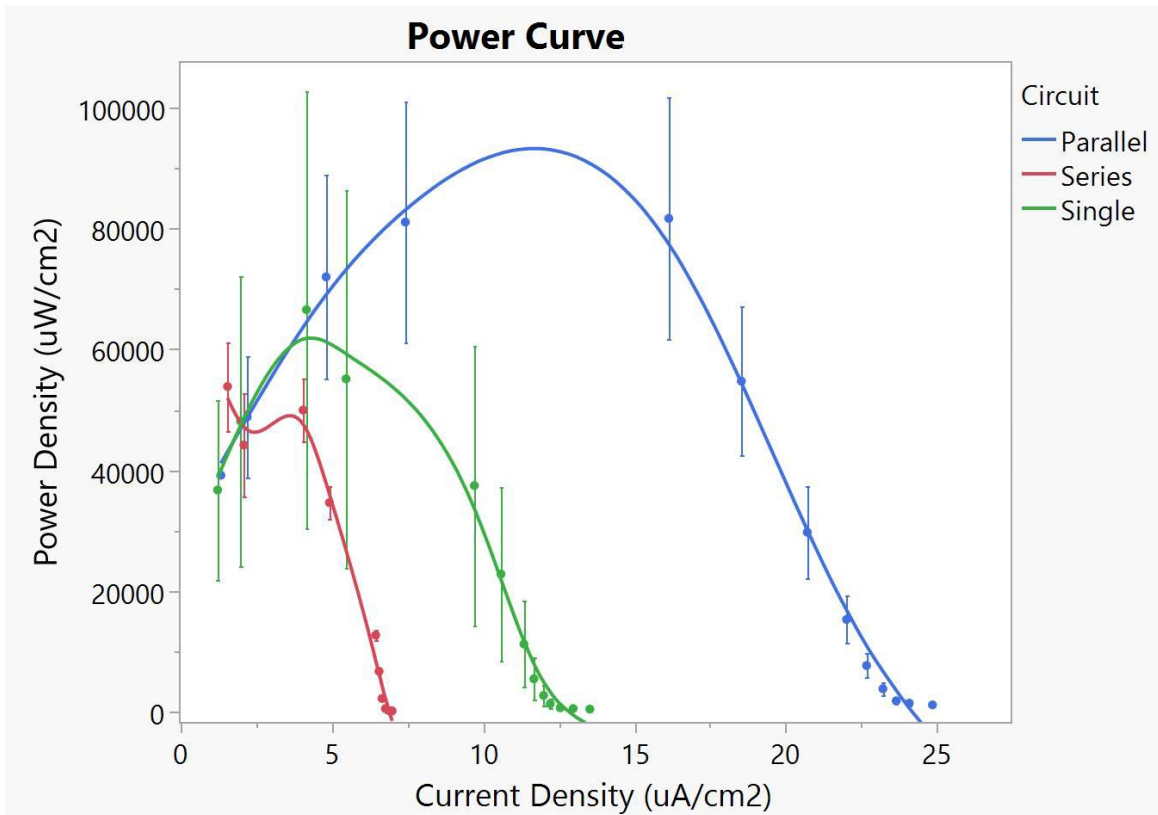


Figure 2.9: Power curve comparing algal fuel cell in parallel, series, and individual configurations.

The power curve showed an analogous trend to OCV where the fuel cells connected in parallel had the highest performance, followed by the individual fuel cells and the fuel cells connected in series. It was noticed that the parallel-connected stack resulted in the highest power density and showed a curve nearest to the expected standard. Since the fuel cell is biological in nature it is difficult to predict the response of the system to testing; and, it is possible that there is some interaction within the fuel cell, such as the biological organisms adapting to drawing currents causing higher capacity for power generation.

3. ELECTROCHEMICAL ANALYSIS OF ALGAL FUEL CELL

3.1 Introduction

In the search to find renewable and sustainable alternatives to the traditional sources of energy, microbial fuel cells are being researched significantly. Although bacteria and fungi are the most popularly used microorganisms in MFCs, algae is used for these tests due to its wastewater treatment efficiency, nutrient content, and power density. One of the challenges of MFCs is its low power output due to biological limiting factors, therefore it is necessary to understand the reactions between the microorganisms and the electrodes to attempt to overcome these factors [48]. One of the limiting factors that need to be investigated is the internal resistance of the fuel cell. Electrochemical Impedance Spectroscopy (EIS) was used to identify and characterize binding events on the electrode and attempt to investigate these limiting factors [49] [50].

It is well known that electrical resistance is the ability of a circuit element to resist the flow of electrical current, and it is defined using Ohm's law as stated previously. However, resistance is not an adequate term to describe the complex behavior that these real-world circuit elements exhibit. Therefore, impedance is used in place of resistance. Impedance still measures the ability of an element to resist electrical current; however, it is not limited by the same properties as resistance. Electrochemical impedance is measured by applying an AC potential to an electrochemical cell and measuring the resulting current through the cell [51]. Since the applied potential is typically sinusoidal, the resulting current is also sinusoidal but with a phase shift. Equation 3 shows the relationship between the applied potential, current and complex impedance responses.

$$E=IZ \quad \text{Equation 3}$$

where: E is the applied sinusoidal potential in volts,

I is the sinusoidal current response in amperes and

Z is the complex impedance in ohms.

The complex impedance, Z , is composed of a real and an imaginary part. Equation 4 shows this relationship.

$$Z = Z_{Re} + Z_{Im}(\omega) \quad \text{Equation 4}$$

where: Z_{Re} is the real impedance corresponding to resistance in ohms and

Z_{Im} is the imaginary impedance due to capacitance in ohms.

The real impedance, which is frequency independent, comes from a few different resistances in the electrochemical cell. The contributions to real impedance are series resistances (R_s), charge transfer resistance (R_{CT}), and mass transfer resistance (R_{mt}) [50]. The imaginary impedance, which is due to capacitance and is frequency dependent, is typically from charging of the electric double layer [52]. The electric double layer is typically represented as a capacitive element in the equivalent circuitry. This occurs at the interface of a conductive electrode and an electrolyte solution. Two layers of opposing polarity form, separated by a single layer of solvent molecules.

A common method to analyze the EIS data is with a Nyquist plot [53]. The Nyquist plot compares the real and the imaginary impedance of the transfer function in response to a frequency sweep [54]. Figure 3.1 shows a typical Nyquist plot for an electrochemical cell similar to testing done here.

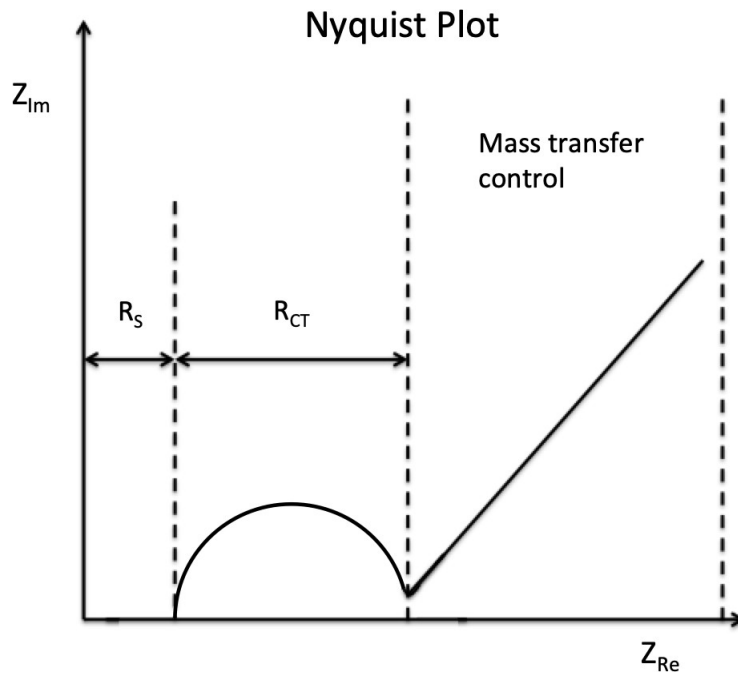


Figure 3.1: Nyquist plot

The first part of the graph, which is at a high frequency, corresponds to the solution resistance, R_s (ohms). As the frequency decreases, the second segment forms the semicircle. The diameter of the semicircle is the charge transfer resistance, R_{CT} (ohms). The resistance of the solution and the charge transfer resistance make up all the internal resistance. The capacitive impedance approaches infinity as the frequency continues decreasing and all current passes via charge and mass transfer. A line at 45° in the low frequency region of the Nyquist plot is indicative of Warburg impedance, Z_w (ohms). This shows that there is semi-infinite linear diffusion, or unrestricted diffusion to a large planar electrode [55].

3.2 Methods and Materials

3.2.1 Electrochemical Impedance Spectroscopy

The algae fuel cell was set up as previously described; the anode was used as the working electrode, the cathode as the counter and reference electrodes. The AC Impedance Parameters used can be found in Table 3.1. The EIS testing was evaluated with a Nyquist plot on days 2, 4, 7, and 9 of the fuel cell in replicate. CH Instruments potentiostat, model number CHI6044E, was used for all data measurements.

Table 3.1: AC Impedance Parameters

Initial E (V)	High Frequency (Hz)	Low Frequency (Hz)	Amplitude(V)	Quiet Time (s)
0.005	100,000	0.01	0.1	10

EIS Spectrum Analyser software [56] was used to find the desired parameters and the best fit.

3.2.2 SEM Images

The bare graphite anode was imaged with Scanning Electron Microscopy (SEM) at 200 μ m and 20 μ m. No coating was necessary since the graphite felt had sufficient charge.

A fuel cell was set up and run, and the anode was removed from the chamber on the seventh day for imaging. The anode with the biofilm was dried overnight at 90°C and coated with gold. It was then imaged using SEM at 200 μ m and 100 μ m.

3.3 Results and Discussion

To further characterize the electrochemical interactions in the fuel cell a Nyquist plot was created (Figure 3.2). Figure 3.2 shows the difference in electrochemical impedance on 4 different days of the algal fuel cell.

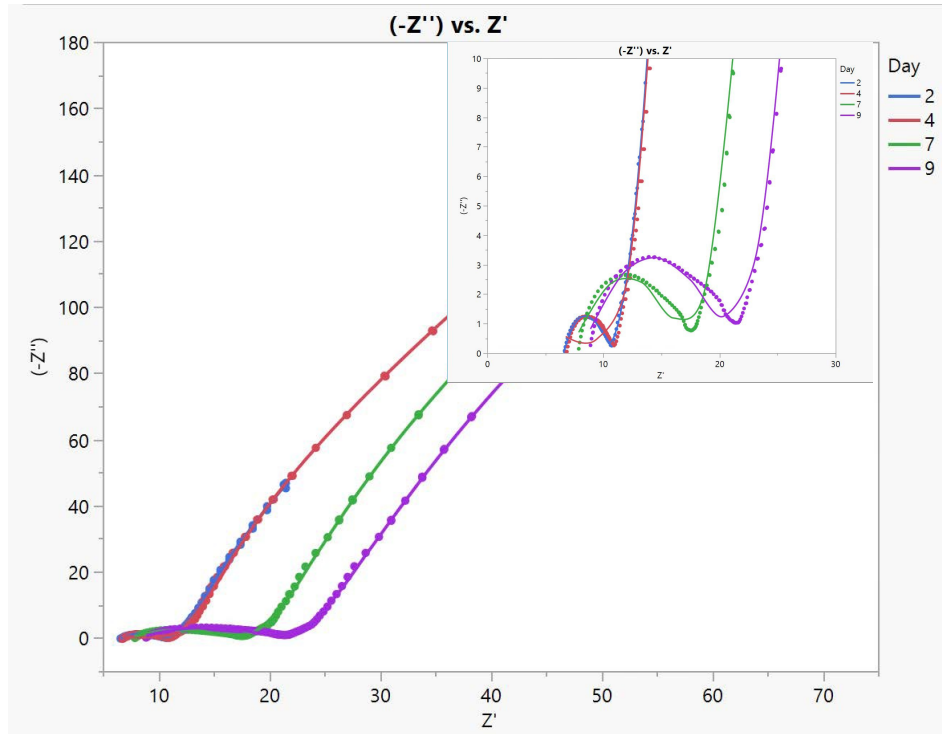


Figure 3.2: Nyquist plots obtained on days 2, 4, 7 and 9 of algal fuel cell testing. Inset picture shows the semi-circle at high frequency range indicating charge transfer resistance.

The resistance of the solution (R_s) increases slightly each day, which is consistent with algal growth in the anode solution. The diameter of the semicircle increases greatly from days 2 and 4 to days 7 and 9. Since the diameter corresponds to the charge transfer resistance (R_{CT}), the increase in diameter means there is an increase in R_{CT} . The charge transfer resistance pertains to the transfer of electrons from one phase to another. This increase in resistance is most likely from the growth of the biofilm on the anode, meaning the transfer is from the biofilm to the anode. The line in the low-frequency range is indicative of a diffusion process. The presence of the Warburg impedance indicates that the fuel source is also diffusion driven. This indicates that algae not only on the biofilm but also in the anode compartment play an active role in the electron transfer process. This observation is important since it is inevitable that algae in the biofilm that is dying can negatively impact the performance of the fuel cell; however, the existence of the diffusion

component implies the ability to extend the operation time of the fuel cell.

The Nyquist plot was fit with equivalent circuitry to find R_s and R_{CT} . The Randles circuit, Figure 3.3, was the best fit found based on the %error.

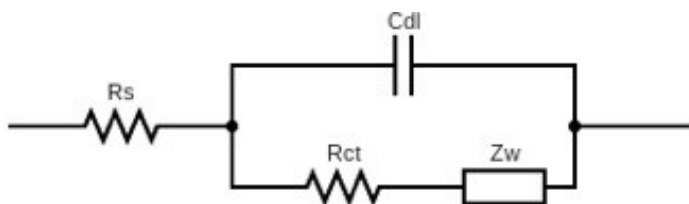


Figure 3.3: Randles circuit showing solution resistance (R_s), charge transfer resistance (R_{CT}), double layer capacitance (C_{dl}) and Warburg impedance (Z_w).

Table 3.2 shows the solution resistance and the charge transfer resistance for each day.

Table 3.2: Solution resistance and charge transfer resistance on days 2, 4, 7 and 9 of an algal-based microbial fuel cell.

Circuit Element	Day 2 (14.80% error)	Day 4 (16.90% error)	Day 7 (14.36% error)	Day 9 (14.50% error)
$R_s(\Omega)$	7.60	7.90	8.63	9.60
$R_{CT}(\Omega)$	2.40	2.35	7.19	9.30
$Z_w(\Omega s^{-1/2})$	5.34	5.86	9.18	10.42

As expected, the resistance of the solution slightly increased each day, while the charge transfer resistance increased significantly. The p-value for both resistances was under 0.0001, demonstrating the significance of the measurement day and the resistances in the system. This fit also showed some error in the slope of the line correlating to the Warburg impedance. A deviation from the typical Warburg effect has been correlated to anomalous diffusion in literature. Increasing roughness of the film causes diffusing particles to become trapped in the media, thus

inducing the anomalous behavior [57]. Anomalous diffusion could be causing the error in this data because the electrode used was macro-porous as seen in Figure 3.4.

Literature does not focus heavily on EIS analysis for algae fuel cell with micro-algae in the anode, most have looked at bacterial fuel cells. The results of the bacterial-MFCs have shown that the resistance of the solution stays relatively the same, ranging from 3 to 25 ohms between studies. However, the charge transfer resistance decreased over an extended period of time (50-300 days) on the scale of thousands of ohms to tens [51]. The difference in values between literature and the experimental data could be due to the difference in microbes, the scale of days measured, or the dimensions of the anode.

3.3.1 Scanning Electron Microscopy images

Scanning Electron Microscopy (SEM) was used to characterize the surface of the anode on the day with the highest OCV. Figure 3.4 shows the bare anode and Figure 3.5 shows the biofilm on the anode after 7 days.

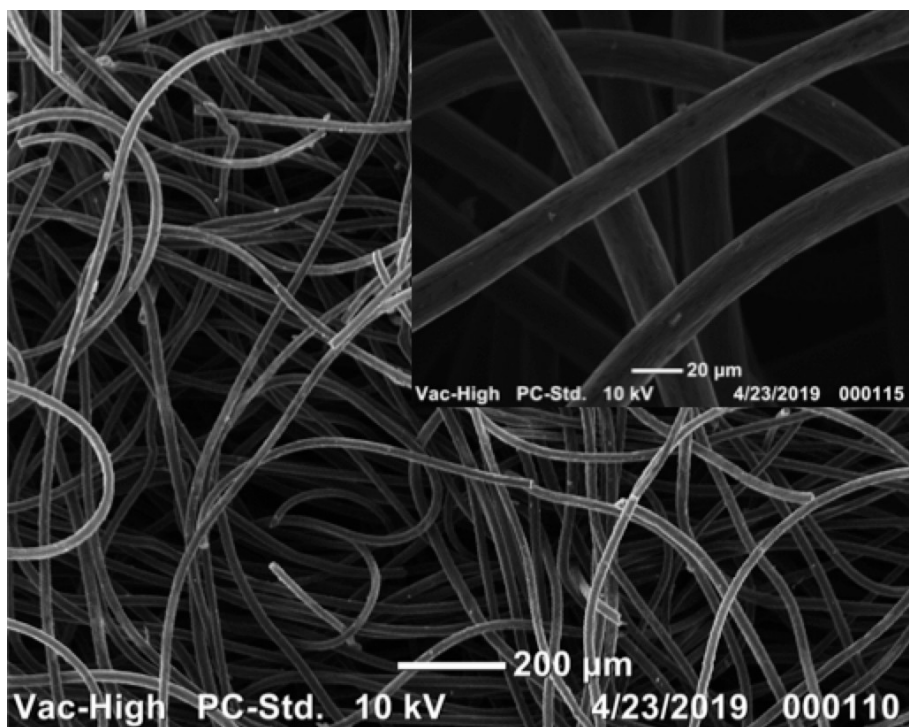


Figure 3.4: SEM image of the bare graphite felt electrode at 200µm and inset shows at 20µm.

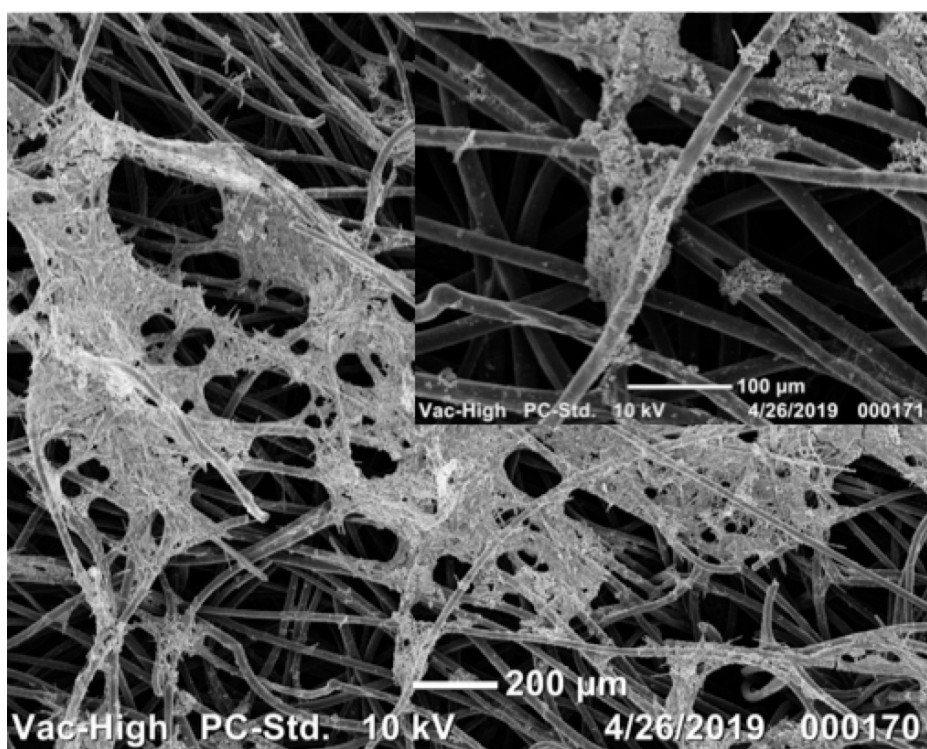


Figure 3.5: (a) SEM image of *Spirulina platensis* biofilm after 7 days of growth on the surface of a graphite felt electrode, coated with gold for imaging at 200µm and the inset at 100µm.

There are some regions on the anode where the microalgae appear to cluster together and form flocs of algae. This shows that the algae does form a good biofilm on the surface of the graphite felt anode.

4. SUMMARY AND CONCLUSIONS

There is a dire need in our world for improved renewable energy practices if we are to keep up with the growing population and the decline in our current fuel sources. One of the potential solutions to this issue is microbial fuel cells. MFCs would be a great solution because they not only produce electricity but they can also treat wastewater or remove heavy metals. Microalgae are promising microbes for MFCs because they are easy to cultivate, produce large amounts of biomass that can be harvested, sequester CO₂ and produce oxygen, and can serve as the primary electron donor in the MFC.

An algae-based microbial fuel cell was designed and developed with the goal of being simple, cost effective and having higher performance. The algae *Spirulina platensis* was selected due to its high nutritional content and ease of cultivation. The growth curve of *Spirulina platensis* showed that re-inoculation with fresh media is optimal after 14 days of growth. Since the initial testing with voltage measurement across the resistor was too low to read, the tests were conducted measuring the voltage in series with the resistors. This showed that the highest potential output came from the algae fuel cell on day 7 ($227.7 \pm 0.0807\text{mV}$), followed by day 9 ($203 \pm 0.06286\text{mV}$) and 4 ($192.7 \pm 0.0476\text{mV}$). Additional testing was done to measure the true output of the fuel cell on the day with the highest performance, day 7. The resistor sweep was performed in series with the system measured with an ammeter. The fuel cell was run individually, in series and parallel. The results showed that output could be improved by connecting the fuel cells in parallel ($59.8 \pm 7.96\text{mW/cm}^2$). Voltage reversal occurred in the series connection likely due to a lower output from one of the cells causing an adverse reaction in the other two.

The EIS testing showed the expected response, that the resistance of the system increases slightly as the fuel cell continues running due to biomass growth, while the charge transfer

resistance increases greatly as the biofilm grows on the anode. An equivalent circuit for this fuel cell was determined to be the Randles circuit which implies resistance in the system due to the resistance of the solution and charge transfer, capacitance from the double layer on the surface of the anode, and from the Warburg element.

4.1 Future Work

There is still much progress that needs to be made to optimize algae-based microbial fuel cells for practical applications. Namely, the power output needs to be increased by reducing the resistances in the system and optimizing the parameters of the fuel cell. Further testing should be done to characterize the binding events of the biofilm on the anode, and to increase the available surface area of the electrode. With a higher available surface area, there will be an increase in electron transfer and higher output power. Another opportunity for further research is the optimization of the fuel cell stacks, to identify the cause of voltage reversal in this system and overcome for increased performance. Lastly, this fuel cell could be tested with wastewater in place of the media to test for practical application in wastewater treatment facilities.

REFERENCES

- [1] C. Robinson, *The Depletion of Energy Resources*, pp. 21–55. London: Macmillan Education UK, 1975.
- [2] D. o. E. United Nations and P. D. Social Affairs, “World population prospects: The 2017 revision, key findings and advance tables,” vol. Working Paper No. ESA/P/WP/248, 2017.
- [3] M. Zhou, H. Wang, D. J. Hassett, and T. Gu, “Recent advances in microbial fuel cells (mfcs) and microbial electrolysis cells (mecs) for wastewater treatment, bioenergy and bioproducts,” *Journal of Chemical Technology Biotechnology*, vol. 88, no. 4, pp. 508–518, 2013.
- [4] Z. Baicha, M. J. Salar-Garcia, V. M. Ortiz-Martinez, F. J. Hernandez-Fernandez, A. P. de losos, N. Labjar, E. Lotfi, and M. Elmahi, “A critical review on microalgae as an alternative source for bioenergy production: A promising low cost substrate for microbial fuel cells,” *Fuel Processing Technology*, vol. 154, pp. 104–116, 2016.
- [5] E. Ogungbemi, O. Ijaodola, F. N. Khatib, T. Wilberforce, Z. El Hassan, J. Thompson, M. Ramadan, and A. G. Olabi, “Fuel cell membranes pros and cons,” *Energy*, vol. 172, pp. 155–172, 2019.
- [6] R. O’hayre, S.-W. Cha, F. B. Prinz, and W. Colella, *Fuel cell fundamentals*. John Wiley Sons, 2016.
- [7] G. F. McLean, T. Niet, S. Prince-Richard, and N. Djilali, “An assessment of alkaline fuel cell technology,” *International Journal of Hydrogen Energy*, vol. 27, no. 5, pp. 507–526, 2002.
- [8] J.-H. Wee, “Applications of proton exchange membrane fuel cell systems,” *Renewable and Sustainable Energy Reviews*, vol. 11, no. 8, pp. 1720–1738, 2007.
- [9] S. Cosnier, A. J. Gross, F. Giroud, and M. Holzinger, “Beyond the hype surrounding bio-

- fuel cells: What's the future of enzymatic fuel cells?," *Current Opinion in Electrochemistry*, vol. 12, pp. 148–155, 2018.
- [10] X. Ren, P. Zelenay, S. Thomas, J. Davey, and S. Gottesfeld, "Recent advances in direct methanol fuel cells at los alamos national laboratory," *Journal of Power Sources*, vol. 86, no. 1, pp. 111–116, 2000.
- [11] X. Li and A. Faghri, "Review and advances of direct methanol fuel cells (dmfcs) part i: Design, fabrication, and testing with high concentration methanol solutions," *Journal of Power Sources*, vol. 226, pp. 223–240, 2013.
- [12] N. V. Rees and R. G. Compton, "Sustainable energy: a review of formic acid electrochemical fuel cells," *Journal of Solid State Electrochemistry*, vol. 15, no. 10, pp. 2095–2100, 2011.
- [13] L. J. Blomen and M. N. Mugerwa, *Fuel cell systems*. Springer Science Business Media, 2013.
- [14] N. Sammes, R. Bove, and K. Stahl, "Phosphoric acid fuel cells: Fundamentals and applications," *Current Opinion in Solid State and Materials Science*, vol. 8, no. 5, pp. 372–378, 2004.
- [15] I. S. Chang, J. K. Jang, G. C. Gil, M. Kim, H. J. Kim, B. W. Cho, and B. H. Kim, "Continuous determination of biochemical oxygen demand using microbial fuel cell type biosensor," *Biosensors and Bioelectronics*, vol. 19, no. 6, pp. 607–613, 2004.
- [16] A. Sekrecka-Belniak and R. Toczywska-Mamiska, "Fungi-based microbial fuel cells," *Energies*, vol. 11, no. 10, p. 2827, 2018.
- [17] R. Kumar, L. Singh, A. W. Zularisam, and F. I. Hai, "Microbial fuel cell is emerging as a versatile technology: a review on its possible applications, challenges and strategies to improve the performances," *International Journal of Energy Research*, vol. 42, no. 2, pp. 369–94,

2018.

- [18] A. Hamnett, "Mechanism and electrocatalysis in the direct methanol fuel cell," *Catalysis Today*, vol. 38, no. 4, pp. 445–457, 1997.
- [19] R. K. Pachauri and Y. K. Chauhan, "Various control schemes of power management for phosphoric acid fuel cell system," *International Journal of Electrical Power Energy Systems*, vol. 74, pp. 49–57, 2016.
- [20] Z. Du, H. Li, and T. Gu, "A state of the art review on microbial fuel cells: A promising technology for wastewater treatment and bioenergy," *Biotechnology Advances*, vol. 25, no. 5, pp. 464–482, 2007.
- [21] A. J. Slate, K. A. Whitehead, D. A. C. Brownson, and C. E. Banks, "Microbial fuel cells: An overview of current technology," *Renewable and Sustainable Energy Reviews*, vol. 101, pp. 60–81, 2019.
- [22] G. Palanisamy, H.-Y. Jung, T. Sadhasivam, M. D. Kurkuri, S. C. Kim, and S.-H. Roh, "A comprehensive review on microbial fuel cell technologies: Processes, utilization, and advanced developments in electrodes and membranes," *Journal of Cleaner Production*, vol. 221, pp. 598–621, 2019.
- [23] U. Schröder, J. Nieben, and F. Scholz, "A generation of microbial fuel cells with current outputs boosted by more than one order of magnitude," *Angewandte Chemie International Edition*, vol. 42, no. 25, pp. 2880–2883, 2003.
- [24] D. R. Bond, D. E. Holmes, L. M. Tender, and D. R. Lovley, "Electrode-reducing microorganisms that harvest energy from marine sediments," *Science*, vol. 295, no. 5554, pp. 483–5, 2002. 1095-9203 Bond, Daniel R Holmes, Dawn E Tender, Leonard M Lovley, Derek R Journal Article Research Support, Non-U.S. Gov't United States Science. 2002

Jan 18;295(5554):483-5. doi: 10.1126/science.1066771.

- [25] B. Min and B. E. Logan, "Continuous electricity generation from domestic wastewater and organic substrates in a flat plate microbial fuel cell," *Environmental Science Technology*, vol. 38, no. 21, pp. 5809–5814, 2004.
- [26] B. R. Ringeisen, E. Henderson, P. K. Wu, J. Pietron, R. Ray, B. Little, J. C. Biffinger, and J. M. Jones-Meehan, "High power density from a miniature microbial fuel cell using shewanella oneidensis dsp10," *Environmental Science Technology*, vol. 40, no. 8, pp. 2629–2634, 2006.
- [27] H. J. Kim, H. S. Park, M. S. Hyun, I. S. Chang, M. Kim, and B. H. Kim, "A mediator-less microbial fuel cell using a metal reducing bacterium, shewanella putrefaciens," *Enzyme and Microbial Technology*, vol. 30, no. 2, pp. 145–152, 2002.
- [28] J. Niessen, U. Schröder, and F. Scholz, "Exploiting complex carbohydrates for microbial electricity generation: a bacterial fuel cell operating on starch," *Electrochemistry Communications*, vol. 6, no. 9, pp. 955–958, 2004.
- [29] L. Huang, J. M. Regan, and X. Quan, "Electron transfer mechanisms, new applications, and performance of biocathode microbial fuel cells," *Bioresource Technology*, vol. 102, no. 1, pp. 316–323, 2011.
- [30] A. Gunawardena, S. Fernando, and F. To, "Performance of a yeast-mediated biological fuel cell," *International journal of molecular sciences*, vol. 9, no. 10, pp. 1893–1907, 2008. 19325724[pmid] PMC2635613[pmcid].
- [31] K. Chojnacka, P. P. Wiczorek, G. Schroeder, and I. Michalak, *Algae Biomass: Characteristics and Applications: Towards Algae-based Products*, vol. 8. Springer, 2018.
- [32] J. C. Pires, "Cop21: The algae opportunity?," *Renewable and Sustainable Energy Reviews*,

vol. 79, pp. 867–877, 2017.

- [33] R. Kakarla, C. Kuppam, S. Pandit, A. Kadier, and J. Velpuri, *Algae—The Potential Future Fuel: Challenges and Prospects*, pp. 239–251. Cham: Springer International Publishing, 2017.
- [34] Z. S. e. a. Lodish H, Berk A, *Molecular Cell Biology.*, vol. 4. New York: W. H. Freeman, 2000.
- [35] B. De Caprariis, P. De Filippis, A. Di Battista, L. Di Palma, and M. Scarsella, “Exoelectrogenic activity of a green microalgae, *Chlorella vulgaris*, in a bio-photovoltaic cells (bpvs),” *Chemical Engineering Transactions*, vol. 38, pp. 523–528, 2014.
- [36] I. Gajda, J. Greenman, C. Melhuish, and I. Ieropoulos, “Self-sustainable electricity production from algae grown in a microbial fuel cell system,” *Biomass and Bioenergy*, vol. 82, pp. 87–93, 2015.
- [37] C. Xu, K. Poon, M. M. F. Choi, and R. Wang, “Using live algae at the anode of a microbial fuel cell to generate electricity,” *Environmental Science and Pollution Research*, vol. 22, no. 20, pp. 15621–15635, 2015.
- [38] S. Madani, R. Gheshlaghi, M. A. Mahdavi, M. Sobhani, and A. Elkamel, “Optimization of the performance of a double-chamber microbial fuel cell through factorial design of experiments and response surface methodology,” *Fuel*, vol. 150, pp. 434–440, 2015. (1) (2) Fuel (Fuel, 15 June 2015, 150:434-440) Publication Type: Academic Journal; Rights: Copyright 2015 Elsevier B.V., All rights reserved.
- [39] H. Liu and B. E. Logan, “Electricity generation using an air-cathode single chamber microbial fuel cell in the presence and absence of a proton exchange membrane,” *Environmental Science Technology*, vol. 38, no. 14, pp. 4040–4046, 2004.

- [40] C.-C. Fu, T.-C. Hung, W.-T. Wu, T.-C. Wen, and C.-H. Su, “Current and voltage responses in instant photosynthetic microbial cells with spirulina platensis,” *Biochemical Engineering Journal*, vol. 52, no. 2, pp. 175–180, 2010.
- [41] M. Shukla and S. Kumar, “Algal growth in photosynthetic algal microbial fuel cell and its subsequent utilization for biofuels,” *Renewable and Sustainable Energy Reviews*, vol. 82, pp. 402–414, 2018.
- [42] D. Strik, H. Terlouw, H. Hamelers, and C. Buisman, “Renewable sustainable biocatalyzed electricity production in a photosynthetic algal microbial fuel cell (pamfc),” *Applied Microbiology Biotechnology*, vol. 81, no. 4, pp. 659–668, 2008.
- [43] C. Rajasekaran, C. M. Ajeesh, S. Balaji, M. Shalini, S. Ramamoorthy, D. Ranjan, D. P. Fulzele, and T. Kalaivani, “Effect of modified zarrouk's medium on growth of different Spirulina strains,” *Walailak Journal of Science and Technology (WJST)*, vol. 13, no. 1, pp. 67–75, 2015.
- [44] M.-J. Song, D.-H. Yun, J.-H. Jin, N.-K. Min, and S.-I. Hong, “Comparison of effective working electrode areas on planar and porous silicon substrates for cholesterol biosensor,” *Japanese Journal of Applied Physics*, vol. 45, no. 9A, pp. 7197–7202, 2006.
- [45] D. Whang, “Amperometric glucose biosensor based on a pt-dispersed hierarchically porous electrode,” *Journal of the Korean Physical Society*, vol. 54, no. 4, 2009.
- [46] S. Konopka and B. McDuffie, “Diffusion coefficients of ferri- and ferrocyanide ions in aqueous media, using twin-electrode thin-layer electrochemistry,” *Analytical Chemistry*, vol. 42, no. 14, pp. 1741–1746, 1970.
- [47] S. E. Oh and B. E. Logan, “Voltage reversal during microbial fuel cell stack operation,” *Journal of Power Sources*, vol. 167, no. 1, pp. 11–17, 2007.

- [48] Z. He and F. Mansfeld, "Exploring the use of electrochemical impedance spectroscopy (eis) in microbial fuel cell studies," *Energy Environmental Science*, vol. 2, no. 2, pp. 215–219, 2009.
- [49] Z. He, Y. Huang, A. K. Manohar, and F. Mansfeld, "Effect of electrolyte ph on the rate of the anodic and cathodic reactions in an air-cathode microbial fuel cell," *Bioelectrochemistry*, vol. 74, no. 1, pp. 78–82, 2008.
- [50] R. P. Ramasamy, Z. Ren, M. M. Mench, and J. M. Regan, "Impact of initial biofilm growth on the anode impedance of microbial fuel cells," *Biotechnology and Bioengineering*, vol. 101, no. 1, pp. 101–108, 2008.
- [51] N. Sekar and R. P. Ramasamy, "Electrochemical impedance spectroscopy for microbial fuel cell characterization," *J Microb Biochem Technol S*, vol. 6, no. 2, 2013.
- [52] H. Monshat, "Carbon nanotube thin film supported by nickel nanotube array as supercapacitor electrode with improved rate capability," *Graduate Theses and Dissertations*, 2016.
- [53] A. K. Manohar, O. Bretschger, K. H. Neilson, and F. Mansfeld, "The use of electrochemical impedance spectroscopy (eis) in the evaluation of the electrochemical properties of a microbial fuel cell," *Bioelectrochemistry*, vol. 72, no. 2, pp. 149–154, 2008.
- [54] H. Dong, H. Yu, X. Wang, Q. Zhou, and J. Feng, "A novel structure of scalable air-cathode without nafion and pt by rolling activated carbon and ptfе as catalyst layer in microbial fuel cells," *Water Research*, vol. 46, no. 17, pp. 5777–5787, 2012.
- [55] A. J. Bard, L. R. Faulkner, J. Leddy, and C. G. Zoski, *Electrochemical methods: fundamentals and applications*, vol. 2. wiley New York, 1980.
- [56] A. Bogomolov, M. Hachey, and A. Williams, "In: Progress in chemometrics research isbn 1-59454-257-0 editor: Alexey I. pomerantsev, pp. 119-135 copyright 2005 nova science pub-

lishers, inc.,” *Progress in chemometrics research*, p. 119, 01 2005.

- [57] A. Sharifi-Viand, M. G. Mahjani, and M. Jafarian, “Investigation of anomalous diffusion and multifractal dimensions in polypyrrole film,” *Journal of Electroanalytical Chemistry*, vol. 671, pp. 51–57, 2012.